BIOCHEMISTRY
including biophysical chemistry & molecular biology

Rapid Report

pubs.acs.org/biochemistry

Competition between Fibrillation and Induction of Vesicle Fusion for the Membrane-Associated 40-Residue β-Amyloid Peptides

Rumonat D. Akinlolu, Mimi Nam, and Wei Qiang*

Department of Chemistry, State University of New York at Binghamton, Binghamton, New York 13902, United States

Supporting Information

ABSTRACT: Disruption of the cell membrane by the β-amyloid (Aβ) peptides has been considered as a main mechanism of Alzheimer's disease. The peptide-to-lipid molar ratio (P:L) varies over a broad range biologically. We report here that two of the previously observed Aβ evolution pathways, fibrillation and induction of vesicle fusion, compete with each other when P:L varies in model Aβ–liposome systems. Fibrillation is preferred at higher P:L values, and fusion is promoted at lower P:L values. Structural studies suggest that the same residues in Aβ may involve in both the initial fibrillation and membrane binding at the fusion sites.

Disruption of the cellular membrane has been proposed as a universal pathological mechanism for amyloid diseases.[1−3] For Alzheimer's disease (AD), the aggregation of β-amyloid (Aβ) peptides has fatal effects on neuronal cell membranes. A number of different evolution pathways have been identified.[1] Among these pathways, fibrillation was observed for a broad range of membrane systems from synthetic liposomes to living cells.[4−8] More recently, a few studies demonstrated that Aβ could be fusogenic, which might provide an alternative mechanism for its neurotoxicity.[9,10] Studies of the Aβ–membrane interactions revealed that the detailed membrane disruption pathways were influenced by a number of factors such as lipid composition, membrane fluidity, and peptide-to-lipid molar ratio (P:L).[8,11−16] Within all these factors, P:L seems to be particularly interesting because other factors may affect the membrane disruption by influencing the Aβ concentration and therefore the value of P:L. For instance, the addition of cholesterol and sphingomyelin, which is known to decrease membrane fluidity, may also lead to the heterogeneous distribution of Aβ within bilayers. The membrane region (known as the "raft") with higher sterol contents may have enriched Aβ.[17] In this work, we observed the competition between fibrillation and vesicle fusion induced by Aβ, which could be modulated by P:L.

Two types of fluorescence assays were utilized to analyze the kinetics of fibrillation and the extent of induced vesicle fusion for the Aβ–liposome systems. The details of the fluorescence assays are given in the Supporting Information. Figure 1A shows that the fibrillation rate decreases at lower P:L values. For these experiments, the peptide concentration was kept at 50 μM for all samples. Therefore, the slower fibrillation kinetics was not due to the dilution of peptides. Figure 1B shows the quantification of vesicle fusion, using doubly fluorophore-labeled vesicles and literature methods.[18,19] The strongest tendency to fuse (i.e., 100

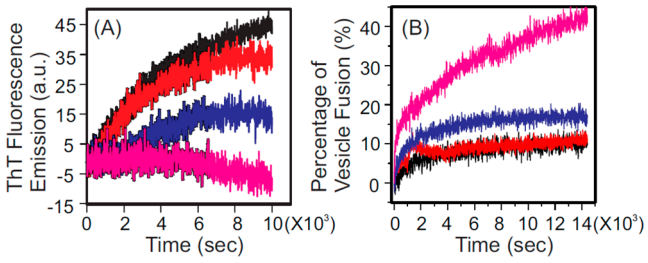

Figure 1. (A) ThT fluorescence assay for measuring the fibrillation kinetics of Aβ–liposome samples with P:L values of 1:30 (black), 1:60 (red), 1:90 (blue), and 1:120 (purple). (B) Fluorescence assay for quantifying the extent of vesicle fusion for the same set of Aβ–membrane samples as in panel A. For both assays, control experiments with only liposomes were performed for each sample.

on the vertical axis of Figure 1B) was obtained by adding 1% Triton X-100 to completely disrupt the vesicles.[18] In general, a lower P:L seems to facilitate vesicle fusion but eliminate fibrillation. The greatest extent of vesicle fusion was observed for the sample with a P:L of 1:120, which did not form fibrils even after a long incubation (i.e., 48 h). Morphologically, the transmission electron microscopy (TEM) images showed more disrupted vesicles after fusion. However, static ^{31}P NMR spectra have shown that the bulk phospholipid bilayer structures were retained (Figure S1 of the Supporting Information). We have also tested the effect of membrane components on fusion for samples with P:L values of 1:120 (Figure S2 of the Supporting Information) and 1:90 (data not shown). It was a general trend that the extent of fusion was lower with either the depletion of negatively charged PG or the addition of cholesterol. For the liquid crystalline phase phospholipid bilayer (the transition temperature (T_c) of the lipids used for the fluorescence assays was −2 °C), the addition of cholesterol is known to increase the rigidity of bilayers. Therefore, lipid mixing may be more difficult with a higher cholesterol fraction.[8] Incorporation of negatively charged PG may promote the absorption of Aβ to the membrane surface, which leads to more efficient interactions.[8,20]

To improve our understanding of the molecular mechanism of the competition between fibrillation and fusion, we performed extensive structural studies using circular dichroism (CD) and solid-state nuclear magnetic resonance (NMR) spectroscopy. The global secondary structure showed mainly random coil for samples with a P:L of 1:100 after incubation for 48 h, which was

Received: March 25, 2015
Revised: May 19, 2015
Published: May 19, 2015

DOI: 10.1021/acs.biochem.5b00321
Biochemistry 2015, 54, 3416−3419

different from the dominant β-strand conformation for samples with a P:L of 1:30 (Figure S3 and Table S3 of the Supporting Information). The CD data suggested that the Aβ did not form fibrils with β-sheet structures at lower P:L values. This conclusion was further supported by a set of solid-state NMR ^{13}C-PITHIRDs-CT experiments[21] with single-site ^{13}C labeling at V18-^{13}C′, A21-$^{13}CH_3$, A30-$^{13}CH_3$, and M35-^{13}C′ (sequences listed in Table S1 of the Supporting Information). These residues are located in the N- or C-terminal β-sheets in most Aβ fibrils.[22−28] However, for samples with a P:L of 1:100, none of these labeled sites showed significant ^{13}C signal decay (Figure S4 of the Supporting Information), which indicated the absence of parallel-in-register β-sheets.[21]

We employed ^{13}C−^{31}P rotational-echo double-resonance (REDOR) experiments to investigate the residue-specific proximity of Aβ to the membrane surface phosphate at fusion sites.[19,29] For these measurements, ether-linked phospholipids were utilized to prevent ^{13}C signal overlap in the carbonyl region in NMR spectra. The lipids 1,2-di-*O*-tetradecyl-*sn*-glycero-3-phosphocholine (DTPC) and 1,2-di-*O*-tetradecyl-*sn*-glycero-3-phosphoglycerol (DTPG) have transition temperatures of 13.8 °C.[30] NMR measurements were performed at ambient temperature to ensure the liquid crystalline phase of bilayers. A set of five Aβ peptides were synthesized with ^{13}C′ labeling at two residues for each sequence (shown in Table S1 of the Supporting Information).

Figure 2 plots the experimental REDOR buildup curves for all the labeled sites, and the representative spectra (with 11.8 and

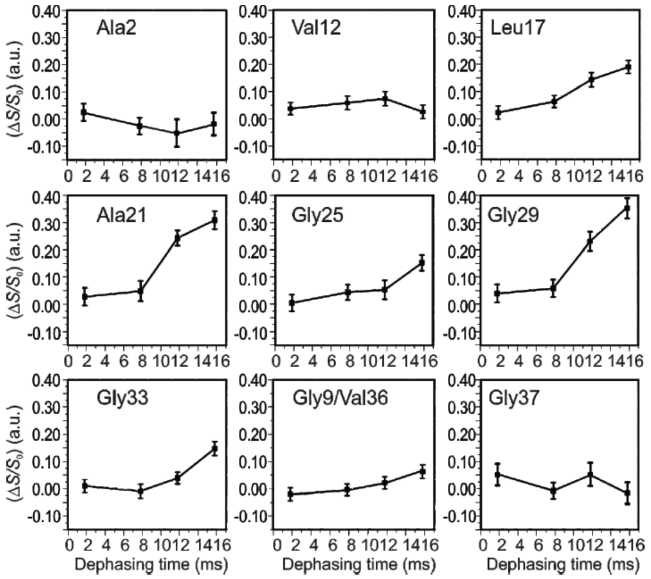

Figure 2. ^{13}C−^{31}P REDOR experimental buildup curves for different singly ^{13}CO-labeled residues within the Aβ−membrane samples with a P:L of 1:100. The sample labeled "G9/V36" indicates the overlap of ^{13}CO signals between the two sites (see the text).

15.8 ms REDOR dephasing times) are shown in Figure S5 of the Supporting Information. For these plots, greater REDOR buildup ($\Delta S/S_0$) indicates shorter internuclear distances between ^{13}C and ^{31}P.[31] These results clearly indicate that certain segments in the Aβ sequence had close interactions with the membrane bilayer surface (i.e., the location of ^{31}P). For instance, residues A21 and G29 have shown obvious experimental REDOR buildup, with $\Delta S/S_0$ values of 0.31 and 0.36 at the longest dephasing time, respectively. Residues L17, G33, and G25 had moderate $\Delta S/S_0$ values of ∼0.15. Other residues, such as A2, V12, and G37, did not show detectable REDOR buildup within 15.8 ms. For the Aβ sequence labeled at G9 and V36, we have observed only one carbonyl peak at ∼172.5 ppm. It is possible that the ^{13}C′ signals from G9 and V36 overlapped with each other. Nevertheless, there was no detectable REDOR buildup for this particular sample, which suggested that neither Gly9 nor Val36 was located close to the ^{31}P. Qualitatively, the REDOR results revealed a general trend that the segment between L17 and G33 had the closest contact with membranes, while the terminal segments were far away. The ^{13}C−^{31}P REDOR measurements were also performed on several singly ^{13}C-labeled samples (including residues A21 and A30) with a P:L of 1:30, where amyloid fibrils were produced (Figure S6 of the Supporting Information). The results showed little REDOR dephasing, which suggested that the bulk Aβ in mature fibrils did not have close contact with membranes.

The REDOR data indicated that segments between L17 and G33 were involved in the membrane interactions at the fusion sites, which might lead to restrictions on its conformation. We conducted two-dimensional (2D) ^{13}C−^{13}C spin diffusion[32] experiments to investigate whether this segment formed a loop as in mature amyloid fibrils. Three scattering uniformly ^{13}C-labeled Aβ peptides were synthesized (sequences listed in Table S1 of the Supporting Information). The 2D experiments were performed with a spin diffusion time of either 10 or 500 ms, which detected intraresidue or long-range ^{13}C−^{13}C correlations, respectively. Figure 3 shows the representative 2D NMR spectra for the sample labeled at D23, S26, K28, A30, and V40. Additional NMR spectra are provided in Figure S7 of the Supporting Information.

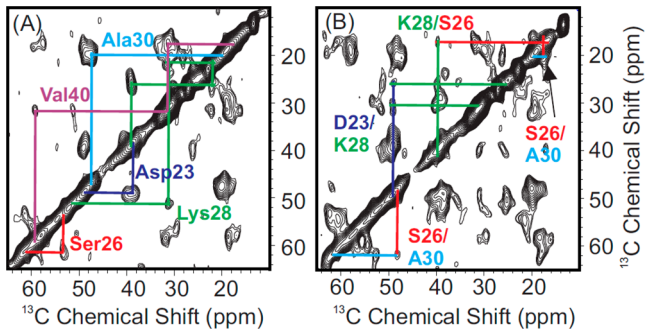

Figure 3. 2D spin diffusion for samples with uniform ^{13}C labeling at D23, S26, K28, A30, and V40 with mixing times of (A) 10 and (B) 500 ms. In panel A, intraresidual cross-peaks are shown with connections and color-coded. In panel B, inter-residual cross-peaks between D23, S26, K28, and A30 are shown with lines and colors.

Several conclusions can be drawn from the 2D solid-state NMR data. First, residues from L17 to the C-terminus showed well-defined structures, which were indicated by one dominant set of chemical shifts for most labeled sites in these regions. F19 showed two sets of Cα/Cβ cross-peaks, and L17 showed a lower-intensity Cα/Cβ cross-peak. Residues at the N-terminus (S9, G8, and F4) did not show strong peaks in 2D spin diffusion experiments. These results suggested that the N-terminal conformation was not well-defined. The ^{13}C chemical shifts are summarized in Table S2 of the Supporting Information, and the plot of secondary structures relative to random coils is shown in Figure S8 of the Supporting Information. Only A21 and A30 exhibit typical secondary chemical shift patterns for a β-strand

DOI: 10.1021/acs.biochem.5b00321
Biochemistry 2015, 54, 3416−3419

with negative deviations for C′ and Cα and a positive deviation for Cβ. This is consistent with the CD result (Figure S3 of the Supporting Information) for samples with a P:L of 1:100, where the dominant random coil conformation was observed. Second, a number of long-range inter-residue interactions were observed for the residues between D23 and A30. For instance, the cross-peak between D23 and K28 and the cross-peak between S26 and A30 will be possible only if the Aβ segment between D23 and A30 adopts a conformation similar to that in mature fibrils. Our 2D NMR data supported the idea that the side chains of D23, S26, K28, and A30 are all oriented inside of the "U-shape" conformational domain. To further confirm the close contacts of these residues, we performed a $^{13}C-^{15}N$ frequency-selective REDOR (*fs*REDOR) experiment to specifically measure the D23 Cδ–K28 Nζ interaction (Figure S9 of the Supporting Information). The strong REDOR buildup fit to a 4.1 ± 0.2 Å internuclear distance with an assumption of a single conformation of Aβ at fusion sites. This distance was slightly longer than the internuclear distance observed for the salt bridge (i.e., 3.5 ± 0.2 Å)[24] but still indicated close contact between the two sites. Alternatively, it is possible that the longer D23 Cδ–K28 Nζ distance represents an ensemble average of multiple populations of Aβ conformations, because the data presented here did not exclude the presence of multiple conformations. Third, the secondary and tertiary structures for the "strand" region are distinct from fibrils. The ^{13}C chemical shifts at low P:L values are significantly different from the shifts at high ratios (i.e., P:L = 1:30 (Table S2 of the Supporting Information)), which suggests that the peptides at fusion sites had distinct conformations. The commonly observed side chain contact between F19 and L34 was not observed for Aβ at fusion sites.[24,27,28] In summary, the NMR results suggested that it was possible to have a dominant "U-shape" domain at fusion sites, and further NMR measurements could provide more quantitative models.

Structural studies of Aβ at the fusion sites revealed the molecular mechanism of the competition between fibrillation and fusion. For the Aβ–liposome system with a P:L of 1:30,[33] fibrils formed by Aβ under this condition adopted dominant parallel-in-register β-sheet structures, which was confirmed by ^{13}C-PITHIRDs-CT measurements on singly ^{13}C-labeled Aβ samples. At this higher P:L, Aβ formed mature fibrils within a time period of 8 days. Both the ^{13}C chemical shifts and $^{13}C-^{13}C$ dipolar coupling measurements suggested that residues A21 and A30 achieved structural convergence more rapidly (within incubation for 48 h) than other residues such as F19, D23, S26, and L34. Therefore, the segments around these two residues may be involved in the initial stage of fibrillation (i.e., nucleation step). To our surprise, these two regions have also had the closest contact with the membrane surface phosphate based on the $^{13}C-^{31}P$ REDOR data (Figure 2). To confirm the residue-specific difference in REDOR dephasing, deconvolution was applied to the doublet $^{13}C'$ peaks shown in Figure S5 of the Supporting Information, and the results were comparable to these obtained with integration (cf. Figure S10 of the Supporting Information). These NMR studies suggest that at the molecular level, the competition between fibrillation and induced vesicle fusion may due to the competition between peptide–peptide and peptide–lipid interactions involving the same segments within the peptide sequence. At higher P:L values, interactions between Aβ peptides are dominant and therefore fibrillation is preferred. At lower P:L values, the peptide is more likely to interact with lipids (cf. Figure 4).

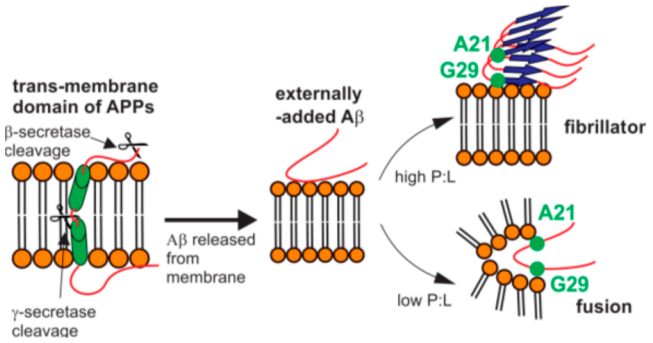

Figure 4. Cartoon models showing the competition between fibrillation and induction of vesicle fusion for the externally added Aβ. Our results show that the segments around A21 and G29/A30 were important for the competition.

The observation of the fibrillation versus fusion competition and its molecular mechanisms have at least two biological ramifications. First, our result suggests that residues around A21 and G29/A30 on Aβ might be important for the initial fibrillation step. Even in the scenario of vesicle fusion, the conformation of residues between E22 and G29 was well-defined. As a comparison, the formation of an H-bond network, which stabilizes the β-sheets in fibrils, may occur in a later stage or may not occur if a competing interaction exists (i.e., peptide–lipid interaction in the case of fusion). Residues A21, E22, and D23 are also frequently involved in the familial mutations of Aβ and their associated familial Alzheimer's disease (FAD).[34] These mutants usually have fibrillation kinetics distinct from those of wild-type Aβ.[35] A possible explanation is that these residues are involved in the initial fibrillation steps. Previous reports of the residue-specific fibrillation kinetics of amylin proposed a similar model in which the connection segments between "loop" and "strands" initiated the fibrillation.[36] More recently, there have been reports of cross-seeding between Aβ and amylin, which might explain the increased risk of developing diabetes for AD patients or vice versa.[37,38] Our results suggested the cross-seeding might be possible because these two amyloid peptides might have similar conformations at the initial fibrillation stage.

Second, our data provide additional information for the amyloid cascade hypothesis (ACH), which is the central hypothesis for explaining the pathology of AD.[39] Recent anti-amyloid drug development based on ACH has shown clear effects on the reduction of Aβ and the elimination of fibrillation. However, these drugs have failed in clinical tests with an only moderate effect on AD progression.[40] Our work indicates that fibrillation might not be the only pathological pathway. In fact, the P:L dependence of fibrillation versus vesicle fusion suggested that at lower Aβ concentrations, the risk of membrane disruption through fusion was even greater. For the strategy of anti-amyloid drug development, further investigation of the detailed interactions that involve the segments around A21 and G29/A30 at the initial stage of fibrillation may be important.

■ ASSOCIATED CONTENT

Supporting Information

Experimental procedures and supplementary figures and tables. The Supporting Information is available free of charge on the ACS Publications website at DOI: 10.1021/acs.biochem.5b00321.

DOI: 10.1021/acs.biochem.5b00321
Biochemistry 2015, 54, 3416–3419

AUTHOR INFORMATION

Corresponding Author

*Department of Chemistry, State University of New York at Binghamton, Binghamton, NY 13902. E-mail: wqiang@binghamton.edu. Telephone: (607) 777-2298.

Author Contributions

R.D.A. and M.N. contributed equally to this work.

Funding

This work is supported by the startup package for W.Q. at the State University of New York at Binghamton and the National Science Foundation Major Research Instrument Foundation (NSF0922815).

Notes

The authors declare no competing financial interest.

ACKNOWLEDGMENTS

We greatly appreciate the help of Dr. Juergen Schulte on NMR experiments. TEM images were recorded in the Analytical and Diagnostic Laboratory at the State University of New York at Binghamton. We acknowledge the help of Dr. In-Tae Bae with TEM.

REFERENCES

(1) Butterfield, S. M., and Lashuel, H. A. (2010) *Angew. Chem., Int. Ed. 49*, 5628−5654.
(2) Eckert, G. P., Wood, W. G., and Muller, W. E. (2010) *Curr. Protein Pept. Sci. 11*, 319−325.
(3) Jelinek, R., and Sheynis, T. (2010) *Curr. Protein Pept. Sci. 11*, 372−384.
(4) Mason, R. P., Estermyer, J. D., Kelly, J. F., and Mason, P. E. (1996) *Biochem. Biophys. Res. Commun. 222*, 72−82.
(5) Müller, W. E., Koch, S., Eckert, A., Hartmann, H., and Scheuer, K. (1995) *Brain Res. 674*, 133−136.
(6) Terzi, E., Holzemann, G., and Seelig, J. (1997) *Biochemistry 36*, 14845−14852.
(7) Widenbrant, M. J., Rajadas, J., Sutardja, C., and Fuller, G. G. (2006) *Biophys. J. 91*, 4071−4080.
(8) Wong, P. T., Shauerte, J. A., Wisse, K. C., Ding, H., Lee, E. L., Steel, D. G., and Gafni, A. (2009) *J. Mol. Biol. 386*, 81−96.
(9) Dante, S., Hauss, T., Brandt, A., and Dencher, N. A. (2009) *J. Mol. Biol. 376*, 393−404.
(10) Vestergaard, M. C., Morita, M., Hamada, T., and Takagi, M. (2013) *Biochim. Biophys. Acta 1828*, 1314−1321.
(11) Williams, T. L., and Serpell, L. C. (2011) *FEBS J. 278*, 3905−3917.
(12) McLaurin, J., and Chakrabartty, A. (1997) *Eur. J. Biochem. 245*, 355−363.
(13) Kremer, J. J., and Murphy, R. M. (2003) *J. Biochem. Biophys. Methods 57*, 159−169.
(14) Lin, M. S. (2007) *Colloids Surf., B 58*, 231.
(15) Sciacca, M. F., Kotler, S. A., Brender, J. R., Chen, J., Lee, D. K., and Ramamoorthy, A. (2012) *Biophys. J. 103*, 702−710.
(16) Qiang, W., Yau, W. M., and Schulte, J. (2015) *Biochim. Biophys. Acta 1848*, 266−276.
(17) Hayashi, H., Mizuno, T., Michikawa, M., Haass, C., and Yanagisawa, K. (2000) *Biochim. Biophys. Acta 1483*, 81−90.
(18) Yang, R., Prorok, M., Castellino, F. J., and Weliky, D. P. (2004) *J. Am. Chem. Soc. 126*, 14722−14723.
(19) Qiang, W., and Weliky, D. P. (2009) *Biochemistry 48*, 289−301.
(20) Bokvist, M., Lindstrom, F., Watts, A., and Grobner, G. (2004) *J. Mol. Biol. 335*, 1039−1049.
(21) Tycko, R. (2007) *J. Chem. Phys. 126*, 064506.
(22) Sgourakis, N. G., Yau, W. M., and Qiang, W. (2015) *Structure 23*, 217−227.
(23) Tycko, R. (2014) *Protein Sci. 23*, 1528−1539.
(24) Lu, J. X., Qiang, W., Yau, W. M., Schwieters, C. D., Meredith, S. C., and Tycko, R. (2013) *Cell 154*, 1257−1268.
(25) Bertini, I., Gonnelli, L., Luchinat, C., Mao, J., and Nesi, A. (2011) *J. Am. Chem. Soc. 133*, 16013−16022.
(26) Qiang, W., Yau, W. M., Luo, Y., Mattson, M. P., and Tycko, R. (2012) *Proc. Natl. Acad. Sci. U.S.A. 109*, 4443−4448.
(27) Paravastu, A. K., Leapman, R. D., Yau, W. M., and Tycko, R. (2008) *Proc. Natl. Acad. Sci. U.S.A. 105*, 18349−18354.
(28) Petkova, A. T., Yau, W. M., and Tycko, R. (2006) *Biochemistry 45*, 498−512.
(29) Qiang, W., Sun, Y., and Weliky, D. P. (2009) *Proc. Natl. Acad. Sci. U.S.A. 106*, 15314−15319.
(30) Ohlsson, G., Tigerstrom, A., Hook, F., and Kasemo, B. (2011) *Soft Matter 7*, 10749−10755.
(31) Gullion, T. (2006) *Mod. Magn. Reson. 1*, 713−718.
(32) Morcombe, C. R., Gaponenko, V., Byrd, R. A., and Zilm, K. W. (2004) *J. Am. Chem. Soc. 126*, 7196−7197.
(33) Qiang, W., Akinlolu, R. D., Nam, M., and Shu, N. (2014) *Biochemistry 53*, 7503−7514.
(34) Benilova, I., Karran, E., and De Strooper, B. (2012) *Nat. Neurosci. 15*, 349−357.
(35) Tycko, R., Sciarretta, K. L., Orgel, J. P., and Meredith, S. C. (2009) *Biochemistry 48*, 6072−6084.
(36) Shim, S., Gupta, R., Ling, Y. L., Strasfeld, D. B., Raleigh, D. P., and Zanni, M. T. (2009) *Proc. Natl. Acad. Sci. U.S.A. 106*, 6614−6619.
(37) Janson, J., Laedtke, T., Parisi, J. E., O'Brien, P., Petersen, R. C., and Bulter, P. C. (2004) *Diabetes 53*, 474−481.
(38) Biessels, G. J., Kappelle, L. J., and Diabetic, U. (2005) *Biochem. Soc. Trans. 33*, 1041−1044.
(39) Hardy, J. A., and Higgins, G. A. (1992) *Science 256*, 184−185.
(40) Karran, E., Mercken, M., and De Strooper, B. (2011) *Nat. Rev. 10*, 698−712.

DOI: 10.1021/acs.biochem.5b00321
Biochemistry 2015, 54, 3416−3419